



**HAL**  
open science

## Monitoring and viscosity identification via temperature measurement on a polymer injection molding line

Qiao Lin, Nadine Allanic, Pierre Mousseau, Manuel Girault, Rémi Deterre

► **To cite this version:**

Qiao Lin, Nadine Allanic, Pierre Mousseau, Manuel Girault, Rémi Deterre. Monitoring and viscosity identification via temperature measurement on a polymer injection molding line. *International Journal of Heat and Mass Transfer*, 2023, 206, pp.123954. 10.1016/j.ijheatmasstransfer.2023.123954 . hal-04061979

**HAL Id: hal-04061979**

**<https://hal.science/hal-04061979>**

Submitted on 20 Nov 2023

**HAL** is a multi-disciplinary open access archive for the deposit and dissemination of scientific research documents, whether they are published or not. The documents may come from teaching and research institutions in France or abroad, or from public or private research centers.

L'archive ouverte pluridisciplinaire **HAL**, est destinée au dépôt et à la diffusion de documents scientifiques de niveau recherche, publiés ou non, émanant des établissements d'enseignement et de recherche français ou étrangers, des laboratoires publics ou privés.

# Monitoring and viscosity identification via temperature measurement on a polymer injection molding line

Qiao Lin<sup>a,\*</sup>, Nadine Allanic<sup>a</sup>, Pierre Mousseau<sup>a</sup>, Manuel Girault<sup>b</sup>, Rémi Deterre<sup>a</sup>

<sup>a</sup> GEPEA Nantes Université, Oniris, CNRS, GEPEA, UMR 6144, F-44000 Nantes, France

<sup>b</sup> Institut PPRIME UPRI CNRS 3346 - CNRS, ISAE-ENSMA, Université de Poitiers ENSMA, Téléport 2, 1 avenue Clément ADER, BP 40109, Futuroscope Chasseneuil CEDEX F-86961, France

## A B S T R A C T

Recent studies emphasize the importance of monitoring equipment/strategy for energy efficiency and quality control of polymer processing. New devices and new methods are proposed for temperature and viscosity measurements on a polymer production line. In this paper, an annular measuring device is used on an injection molding machine to detect material changes through temperature measurement. When the material becomes more viscous, the melt temperature increases due to the viscous dissipation in the production line. An original inverse method based on the viscous dissipation phenomenon is proposed for viscosity identification using temperature measurements of the annular device. The identification process successfully distinguishes the difference in viscosity between two different polymers, and the identification results are in good agreement with other viscosity curves available from the literature.

© 2023 Elsevier Ltd. All rights reserved.

## 1. Introduction

In polymer production, the melt temperature and viscosity are important physical quantities for quality control and for reducing energy consumption [1–4]. Moreover, these physical quantities depend on the processing parameters and the composition of the melt. Production monitoring equipment and on-line/in-line characterization techniques are required. Although different studies have proposed technologies such as ultrasound, dielectric spectroscopy, magnetic resonance, NIR spectroscopy, etc., due to their difficulties in being calibrated and inserted into tools, they are not popular choices in industrial applications. The most commonly used sensors on a polymer production line are still thermocouples and pressure sensors [5].

Various thermocouple-based devices have been designed for production monitoring. Slit or capillary ducts with thermocouples installed on the wall do not disturb the polymer flow passing through the ducts [6,7]. However, wall-mounted thermocouples can be insensitive to the melt temperature [8]. The thermocouple mesh [9] measures the melt temperature at different radial positions with a fast response time thanks to the thin but fragile structure [10]. The thermal measurement cell [11] also performs radial

temperature measurements with a more solid structure and more disturbance to the flow [12].

Temperature measurement is not only useful for production monitoring but also important when identifying viscosity. Viscous dissipation, caused by shear in the flow, can affect the temperature field of the polymer melt and the identification result [11]. Most on-line/in-line viscosity identification techniques employ classical rheometric geometries such as capillary die [13] or slit die [14] with pressure sensors. Some studies suggest using temperature variation due to viscous dissipation as information for viscosity identification [15,16]. However, intrusive thermocouple measurements, having greater sensitivity to melt temperature compared to wall-mounted thermocouples, may disturb the flow field and make it impossible to apply classical rheological geometry models for viscosity identification.

The annular measuring device [17] (TRAC : Thermo-Rheo Annular Cell) is designed to work with an axisymmetric flow model for viscosity identification during polymer production [18]. On the one hand, the polymer flow passing through the annular geometry results in an informative and modelable viscous dissipation concentration around the central axis, and on the other hand, the temperature measurements by thermocouples mounted on the central axis are surrounded by the flow of polymer melt and are protected against thermal disturbances coming from the outer wall of the device. The TRAC has shown its ability to measure small temperature

variations caused by changes in production parameters (plasticization condition, thermal regulation of the barrel, cycle time, etc.) [17].

In this study, the TRAC is used as a monitoring tool on an injection molding machine to detect material changes through temperature measurement. An original inverse method, based on the viscous dissipation phenomenon described in [18], is proposed for viscosity identification using temperature measurements of the TRAC on two different polymers : Polypropylene (abbreviation : PP) and Polystyrene (abbreviation : PS).

## 2. Experimental setup

### 2.1. Instrumented annular duct

The annular measuring device (Fig. 1) used in this study is the same as the one in [17]. It has thermocouples  $T_{1-4}$  installed on the surface of the central axis for melt temperature measurement. Thermocouples  $T_{5-8}$  are on the outer surface of the duct for thermal regulation. All thermocouples are type K. The device is also equipped with two pressure sensors KISTLER 6159A ( $P_1$  and  $P_2$ ) to measure the pressure drop of the flow. The inlet is on the left side in Fig. 1.

More details on the positioning of the sensors, dimensions of the duct, technical solutions, etc. can be found in [17].

### 2.2. Injection machine and data acquisition equipment

The injection molding machine is « MILACRON ELEKTRON 50 » with injection unit « IU-300 ». The maximal injection volume is  $113 \text{ cm}^3$  and the maximal flow rate is  $117 \text{ cm}^3 \cdot \text{s}^{-1}$ . In reality, the entire stroke of the screw (160 mm) is not used. Therefore, the actual volume per injection is below  $113 \text{ cm}^3$ . The maximal plasticization rate is  $18 \text{ g} \cdot \text{s}^{-1}$  ( $20 \text{ cm}^3 \cdot \text{s}^{-1}$  for a polymer with a density of  $900 \text{ kg} \cdot \text{m}^{-3}$ ).

In this study, the mold is removed. The TRAC is mounted at the outlet of the injection unit (Fig. 2). The polymer melt from the injection unit passes through the TRAC and is expelled into the open air (air shot) at the outlet of the TRAC. The signals of the thermocouples and the pressure sensors are gathered. We would like to mention that the TRAC is initially designed to replace the injection nozzle for in-line measurements.

National Instruments « PXIe-1073 » is used to record signals, with « PXIe-4353 » module connected to « TB-4353 » for thermocouples and « PXI-6220 » module connected to « SCB-68 » for pressure sensors.

### 2.3. Typical measurement result on an injection molding machine

To facilitate the understanding of the figures that contain temperature and pressure measurements by the TRAC on an injection molding machine, a typical result is presented in this section with

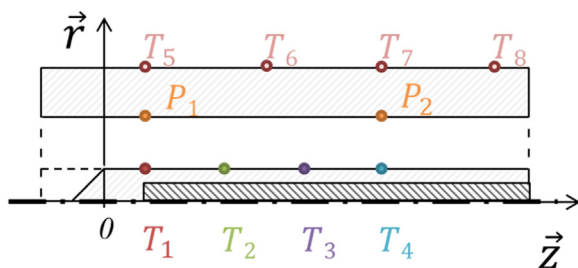


Fig. 1. Schematic diagram of the TRAC (Thermo-Rheo Annular Cell) with sensors labeled.

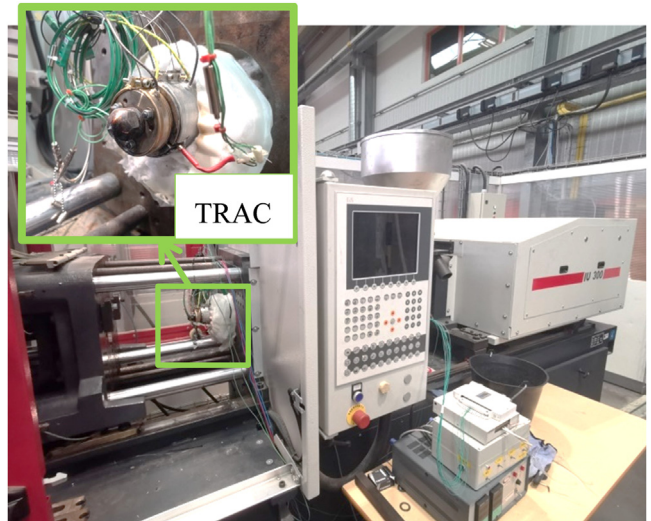


Fig. 2. TRAC mounted at the outlet of the injection unit.

explanations of different characteristic parts of the measurement result.

Fig. 3 contains a classic plasticization-air shot cycle of the injection machine. During the plasticization stage, the screw rotates to plasticize and send the material downstream while moving itself back upstream in the barrel. When there is enough material accumulated in the space downstream of the screw, the plasticization stage ends. During the injection stage, the screw performs a linear motion in the axial direction and pushes the material out of the barrel like a piston.

Index I in Fig. 3 shows a slight increase in pressure during the plasticization stage. The value of this pressure depends on the back pressure setting of the machine. Indeed, the pressure downstream of the screw increases when the screw rotates and sends the material downstream. When the pressure (measured by a machine sensor downstream of the screw) reaches the back pressure setpoint, the screw moves back linearly (upstream) to increase the space downstream between the screw and the barrel in order to regulate the pressure (measured by the machine sensor downstream of the screw) around the back pressure setpoint. This is why the pressure measured during the plasticization is not very stable. The measured temperatures vary little during the plasticization in this test configuration.

Index II in Fig. 3 shows the air shot stage, where the pressure rises sharply, reaches a plateau and then drops rapidly. Depending

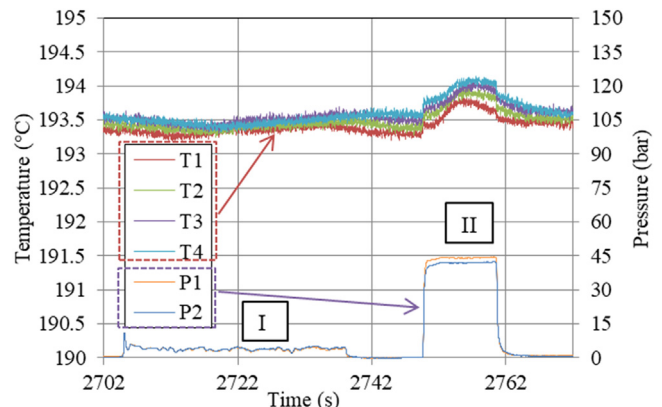


Fig. 3. Temperature and pressure measurements by the TRAC on an injection machine.

on production settings and material condition, the plateau may become a curve. During the air shot, the temperatures measured on the central axis vary. This can be caused by the viscous dissipation in the TRAC or by the material entering the TRAC at a temperature different from that of the central axis [17].

Between the plasticization stage (index I in Fig. 3) and the air shot stage (index II in Fig. 3), a dwell can be added so that the temperature field of the plasticized material can be homogenized in the barrel. In a real injection cycle, there may be a packing stage during which the screw continues to apply pressure to the material after filling the mold. The pressure sensors in the TRAC, positioned downstream of the screw and upstream of the mold, should measure a packing pressure after injection. In our case, as the mold is removed, there is no packing stage. After the air shot, the pressure drops to zero in Fig. 3 (index II in Fig. 3).

### 3. Monitoring

Tests are carried out to see whether the TRAC is capable of detecting a change in material during production by directly reading temperature measurements. During these tests, the setpoint temperature is at 195 °C. The injection molding machine performs successive air shot cycles. In each cycle, we have the following actions:

1. Plasticization at 60 rpm (screw rotation speed) with a back pressure of 2 bar;
2. 10-s pause before each air shot;
3. Air shot at 10 mm.s<sup>-1</sup> (screw translation speed) over 112 mm of stroke (i.e. 7.07 cm<sup>3</sup>.s<sup>-1</sup> for a volume of 79.17 cm<sup>3</sup>);
4. 15-s pause after each air shot.

Although the mold is removed during these tests, pauses are added in the action cycles to simulate the time spent during the packing and cooling stages in real production. The measurements of the TRAC are shown in Fig. 4. For an easy reading of the figure, only the temperatures measured by thermocouples  $T_1$  and  $T_4$  are presented with the pressure measurements of sensors  $P_1$  and  $P_2$ . It should be noted that the temperature measurements on the central axis are protected from external thermal disturbances thanks to the surrounding polymer flow as a barrier [17]. During the plasticization, the polymer in the TRAC almost stops flowing and the temperature measurements are susceptible to external disturbances.

The material initially in the injection molding machine is Polypropylene (TotalEnergies PPC 9642). About thirty cycles are carried out to stabilize the system. Then, Polystyrene (ATOFINA LACQRENE® 1540) is added to the injection molding machine's hopper without interrupting the air shot cycles (Fig. 4a). The PS in the hopper takes several cycles to pass through the barrel and reach the TRAC, so the last cycle of Fig. 4a is still an air shot cycle with PP. The PP air shot cycles continue on the missing timeline between those of Fig. 4a and b. Ten cycles after the addition of PS, a change in the appearance of the material at the outlet of the TRAC is observed. This appearance changing cycle corresponds to the 3rd cycle in Fig. 4b, in which the air shot cycles are numbered. Fig. 4b shows a transient state as PS entering the TRAC. The appearance changing of plastics is shown in Fig. 5, with the same numbering related to that of Fig. 4b.

After the addition of PS in the continuous air shot cycles of PP, the variation in appearance of the recovered plastics at the outlet of the nozzle (Fig. 5) is consistent with the variation in the pressure measured by the TRAC (starting from the 3rd cycle in Fig. 4b). The amplitude of the temperature variation during each air shot increases. This is consistent with the increasing amplitude of the pressure variation, because Polystyrene (ATOFINA LACQRENE® 1540) is more viscous than Polypropylene (TotalEnergies PPC 9642).

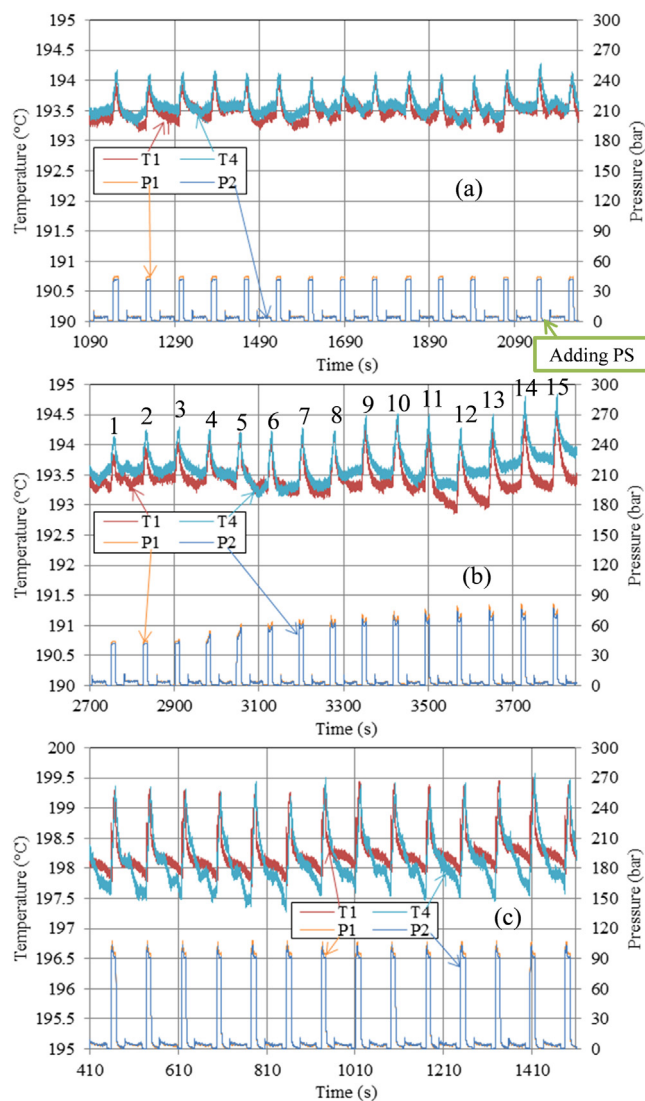


Fig. 4. Air shot cycles (a) with PP, (b) with PP-PS blend and (c) with PS.

Fig. 4c represents air shot cycles with pure PS. We restart a new measurement timeline in Fig. 4c, because it takes a long time to flush the PP with the PS and make sure there is no PP residue in the injection molding machine. We can see that the PS has higher melt temperature, higher pressure and higher temperature spikes during the air shot cycles than the PP, when comparing Fig. 4c-a. This increase in melt temperature and temperature spike amplitude is related to the fact that the PS causes more viscous dissipation, both in the TRAC and in the barrel during plasticization. In these two cases, the temperature measurement can be correlated to the change of material in the production line. It is therefore possible to use thermocouples, which are less expensive and require less strict operating conditions than pressure sensors, to perform this type of process monitoring, provided that these thermocouples are installed within the flow (for example, on the central axis of an annular geometry) to have sufficient measurement sensitivity.

Fig. 6a -c represents the 1st, the 4th and the 15th air shot cycles of Fig. 4b. Fig. 6d is an air shot cycle of pure PS. The interest of pressure sensors is shown in Fig. 6a -c, as the pressure measurement makes it possible to detect variations instantaneously during an air shot, compared to the temperature measurement which has a longer time constant. During the air shots, there is a pressure

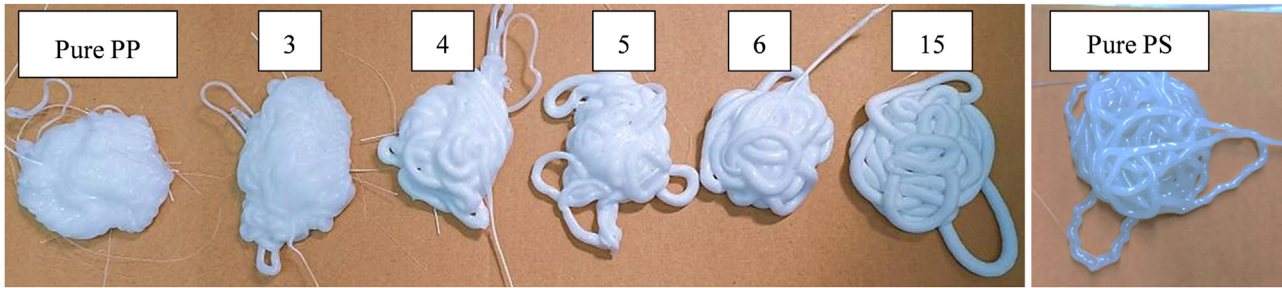


Fig. 5. Appearance of air shot plastics.

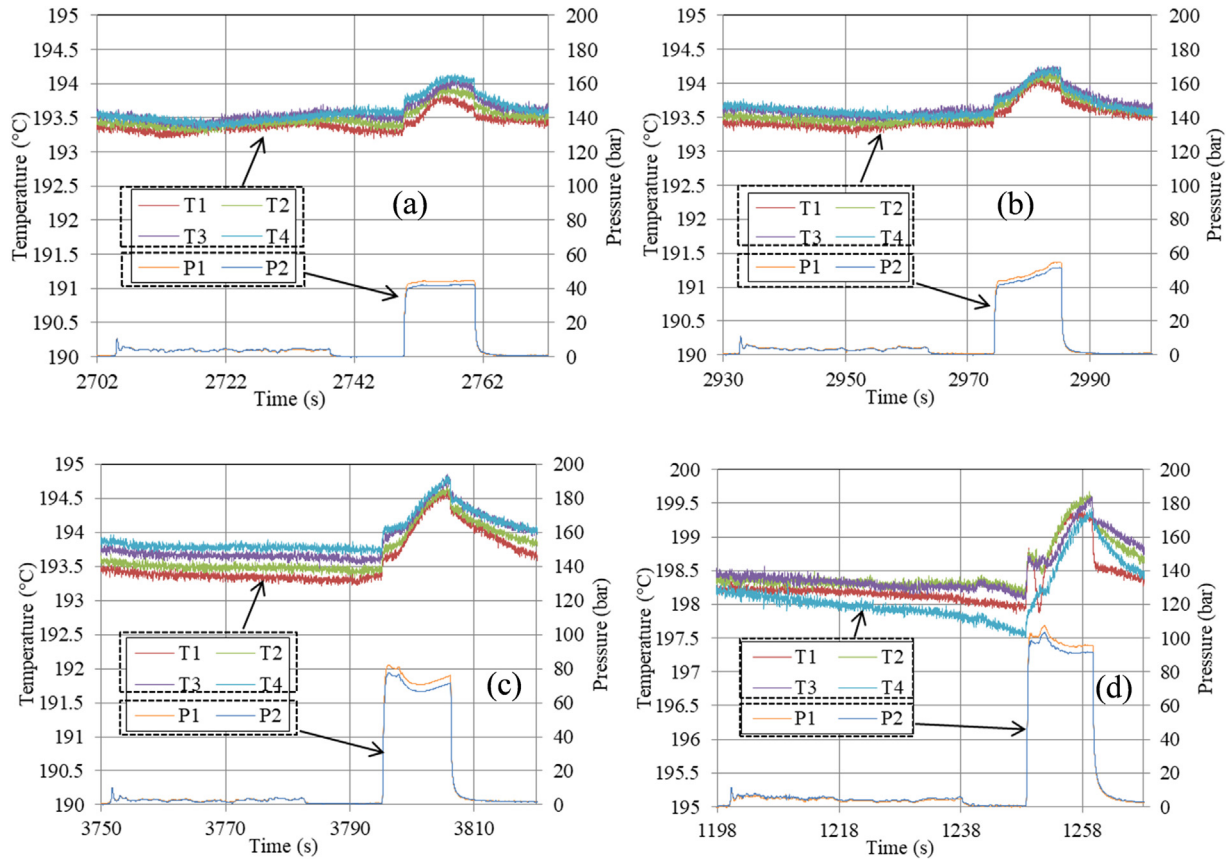


Fig. 6. Air shot of (a) the 1st, (b) the 4th and (c) the 15th cycles of Fig. 4b; (d) air shot of pure PS.

plateau in Fig. 6a, a pressure ramp in Fig. 6b and a more complex pressure curve in Fig. 6c. In Fig. 6d, a temperature fluctuation is detected at the beginning of the air shot. This temperature fluctuation occurs at the same time as the pressure fluctuation measured by the pressure sensors. A possible explanation is that relatively cold material enters the TRAC and increases the pressure due to the temperature dependence of viscosity.

#### 4. Inverse characterization method for viscosity identification

In the inverse characterization process based on the phenomenon of viscous dissipation [18], temperature data measured during an air shot is used to identify the viscosity. Precisely, the central axis generates viscous dissipation in the flow when the polymer melt passes through the TRAC. The temperature variation measured on the central axis can be correlated to the viscosity of the flow. Before introducing the viscous dissipation method, a di-

rect model needs to be defined to simulate an air shot/injection through the annular geometry.

##### 4.1. Direct model

The direct model for the inverse method is slightly different from the one used in the previous study [17]:

- The initial temperature field and the Dirichlet conditions are determined by interpolation of the measurements of the thermocouples.
- The thermal conductivity, the density and the isobar specific heat capacity of the fluid domain are constant and are those of the database of the « Autodesk® Moldflow® » software at the regulation temperature of the injection molding machine.

The direct model [17] is designed to be close to the reality. However, it assumes that inlet temperature is constant. For the inlet temperature to be stable over time during an air shot, the plas-

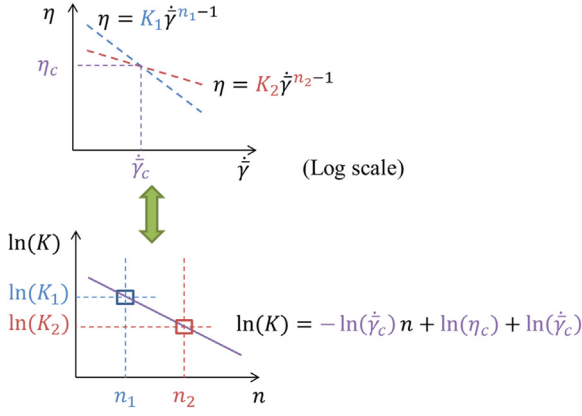


Fig. 7.  $[\dot{\gamma}, \eta]$  space and  $[n, \ln(K)]$  space conversion.

tization stage of the experiments is carried out with a slow rotation speed of the screw (20 rpm). The plasticized material therefore does not heat up too much due to the viscous dissipation in the barrel and has enough time for the temperature field to become uniform before the air shot.

The power law (Eq. (1)) [19,20] is used to describe the rheological behavior of the polymer melt in the direct model,

$$\eta = K\dot{\gamma}^{n-1} \quad (1)$$

with  $\eta$  the viscosity and  $\dot{\gamma}$  the generalized shear rate. Nevertheless, the end result obtained by the viscosity identification method described in the next section is not a power-law curve, but a set of viscosity points for different shear rate values. The power-law modeling is for intermediate steps of the method.

#### 4.2. Viscous dissipation method

This section is based on the phenomenon of viscous dissipation described in the previous research (Section 3.1 of [18]).

If the temperature of the polymer melt entering the TRAC is very different from the temperature of the central axis, the temperature variation on the central axis will be mainly caused by the flow-axis convective exchange, induced by the temperature of the polymer melt, and the information of the viscous dissipation will be masked. When the inlet temperature of the polymer melt is close to the temperature of the central axis, the phenomenon of viscous dissipation is dominant to cause the temperature variation on the central axis. The temperature variation measured on the central axis, due to the viscous dissipation in the flow, can be exploited to obtain a critical point  $(\dot{\gamma}_c, \eta_c)$  on the viscosity curve of the polymer for each air shot [18].

There are different ways to design the algorithm of the identification process. Knowing that the same temperature measurements on the central axis for a given flow rate lead to an infinity of possible power-law curves, passing through a common point: the critical point  $(\dot{\gamma}_c, \eta_c)$  [18], the strategy here is to identify two different power-law curves and find out the intersection (Fig. 7).

In the previous research [18], the  $[n, \ln(K)]$  space is used to perform analysis. The critical point  $(\dot{\gamma}_c, \eta_c)$ , can be transformed into a straight line in the  $[n, \ln(K)]$  space Fig. 7) according to Eq. (2), which is in fact the power law ((1) on a logarithmic scale with  $\ln(K)$  and  $n$  as variables. The straight line in the  $[n, \ln(K)]$  space represents also an isovalue line of the temperature measurement.

$$\ln(K) = -\ln(\dot{\gamma}_c)n + \ln(\eta_c) + \ln(\dot{\gamma}_c) \quad (2)$$

Consequently, the identification of a critical point can be achieved via the identification of a line in the  $[n, \ln(K)]$  space.

These are just two different mathematical points of view of the same calculation process. The identification process of a critical point is thus:

1. Temperature measurements for an air shot at a given flow rate (index II of Fig. 3)
2. Define the cost function  $J_v$  as Eq. (3),

$$J_v = \frac{\sum_{j=1}^{N_t} \sum_{i=1}^{N_{Th}} (T_{i,j} - T_{i,j}^*)^2}{N_{Th}N_t} \quad (3)$$

with  $N_{Th}$  the number of thermocouples,  $N_t$  the number of registered instants,  $T_{i,j}$  the temperature calculated from the direct model and  $T_{i,j}^*$  the temperature measured by thermocouple number  $i$  at time number  $j$ .

3. Find the value of  $K_1$  which minimizes the cost function  $J_v$  by inverse method, with the value of  $n_1$  fixed
4. Find the value of  $K_2$  which minimizes the cost function  $J_v$  by inverse method, with the value of  $n_2$  fixed
5. By injecting the values of  $(n_1, \ln(K_1))$  and  $(n_2, \ln(K_2))$  into Eq. (2), identify the critical point  $(\dot{\gamma}_c, \eta_c)$  with Eqs. (4) and (5).

$$\dot{\gamma}_c = \exp\left(\frac{\ln(K_1) - \ln(K_2)}{n_2 - n_1}\right) \quad (4)$$

$$\eta_c = \exp\left(\frac{\ln(K_1) - \ln(K_2)}{n_2 - n_1}n_1 + \ln(K_1) + \frac{\ln(K_2) - \ln(K_1)}{n_2 - n_1}\right) \quad (5)$$

$n_1$  and  $n_2$  are fixed at 0.3 and 0.5 in the method, because this interval is close to the values of  $n$  for materials commonly used in injection molding [21]. The fact of taking this relatively small interval makes it possible to limit the error of the viscosity identification in the case where the isoline of the temperature in the  $[n, \ln(K)]$  space is not quite a straight line, because of possible neglected phenomena in our model [18]. This is equivalent to a linearization in a small interval.

##### 4.2.1. Sensitivity of critical point calculation to estimation errors of $K_1$ and $K_2$

To study the estimation error of the mentioned identification process, we introduce an error factor  $x$  on the estimation of  $K_1$ . We denote the erroneous critical shear rate as  $\dot{\gamma}_c^*$ , when having  $xK_1$  instead of  $K_1$  in Eq. (4). The critical shear rate shift on a logarithmic scale due to the estimation error is defined as  $\Delta \ln \dot{\gamma}_c$  (Eq. (6)).

$$\Delta \ln \dot{\gamma}_c = \ln \dot{\gamma}_c^* - \ln \dot{\gamma}_c = \frac{\ln x}{n_2 - n_1} \quad (6)$$

$\eta_c^*$  is the erroneous critical viscosity, by using  $xK_1$  instead of  $K_1$  in Eq. (5). The critical viscosity shift on a logarithmic scale can be written as Eq. (7).

$$\Delta \ln \eta_c = \ln \eta_c^* - \ln \eta_c = (n_2 - 1) \Delta \ln \dot{\gamma}_c \quad (7)$$

Using the same principle, when we have  $xK_2$  instead of  $K_2$  in Eqs. (4) and (5), the critical point shift is described by Eqs. (8) and (9).

$$\Delta \ln \dot{\gamma}_c = -\frac{\ln x}{n_2 - n_1} \quad (8)$$

$$\Delta \ln \eta_c = (n_1 - 1) \Delta \ln \dot{\gamma}_c \quad (9)$$

We choose to express the critical viscosity shift in the form of Eqs. (7) and (9), because the power law (1) can also be transformed into a similar differential form as Eq. (10).

$$\Delta \ln \eta = (n - 1) \Delta \ln \dot{\gamma} \quad (10)$$

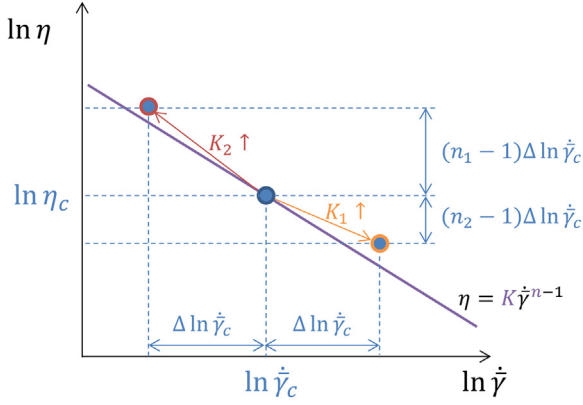


Fig. 8. Critical point shift in case of overestimation of  $K_1$  or  $K_2$ .

Eq. (10) represents a linear relationship between  $\Delta \ln \eta$  and  $\Delta \ln \dot{\gamma}$ . This linear relationship having a slope of  $(n - 1)$  is in fact the power law having an index  $n$  on a logarithmic scale. If the values of  $n_1$  and  $n_2$  are close to that of  $n$ , Eqs. (7) and (9) become almost Eq. (10). That is to say, the estimation errors shift the critical point in a direction close to the slope of the power law. Despite the estimation errors, the critical point will always be close to the sought viscosity curve. It is therefore advantageous to choose values of  $n_1$  and  $n_2$  close to the value of  $n$  of the power law to be identified (if  $n$  can be roughly pre-estimated).

An example is given in Fig. 8 for a shear-thinning material ( $n < 1$ ). An overestimation of  $K_1$  leads to an overestimation of  $\dot{\gamma}_c$  and an underestimation of  $\eta_c$ , with a slope of  $(n_2 - 1)$ . An overestimation of  $K_2$  corresponds to an underestimation of  $\dot{\gamma}_c$  and an overestimation of  $\eta_c$ , with a slope of  $(n_1 - 1)$ .

#### 4.2.2. Influence of the inlet temperature uncertainty

We remind that this method of viscous dissipation is valid when the phenomenon of viscous dissipation is dominant, compared to the phenomenon of convection [18]. That is, when the temperature of the central axis is close to the inlet temperature of the flow. In reality, it is difficult to precisely control the melt temperature on a production line. A shift in the inlet temperature causes extra convective exchange between the flow and the central axis. This extra convective exchange can bend the temperature isolines in the region where the values of  $K$  and  $n$  are small (« Convection dominant zone » [18]), i.e. for less viscous materials generating less viscous dissipation.

To better visualize this « bending effect », a campaign of numerical simulations is performed under the same conditions as those of the previous research (Fig. 3 of [18]), but with an one-degree perturbation on the inlet temperature. The variation of temperature at the end of a two-second injection (at  $30 \text{ cm}^3 \cdot \text{s}^{-1}$ ) compared to the initial temperature field is noted as  $\Delta T$ . The isolines of  $\ln(\Delta T)$  for thermocouples  $T_{1-4}$  are shown in Fig. 9.

In Fig. 9, it is confirmed that the measurements of thermocouples  $T_{1-4}$  give almost the same critical shear rate (slope of the « straight part » of the isoline, see Eq. (2)) on viscous dissipation [18] and that the further downstream the thermocouple is, the less it is influenced (less curved isoline) by convection caused by the inlet temperature offset (coherent with the results of the convection study in [22]), especially if we observe the isolines passing through the circled reference point ( $\ln(K) = 6.0625$  and  $n = 0.6$ ). Thanks to the fact that these two phenomena (viscous dissipation and convection) do not have the same sensitivity distribution on all thermocouples, it is possible to determine the inlet temperature and the value of  $K$  at the same time in the inverse method (instead of entering an arbitrary inlet temperature in the direct model). In this paper, the inlet temperature  $T_{in}$  is considered con-

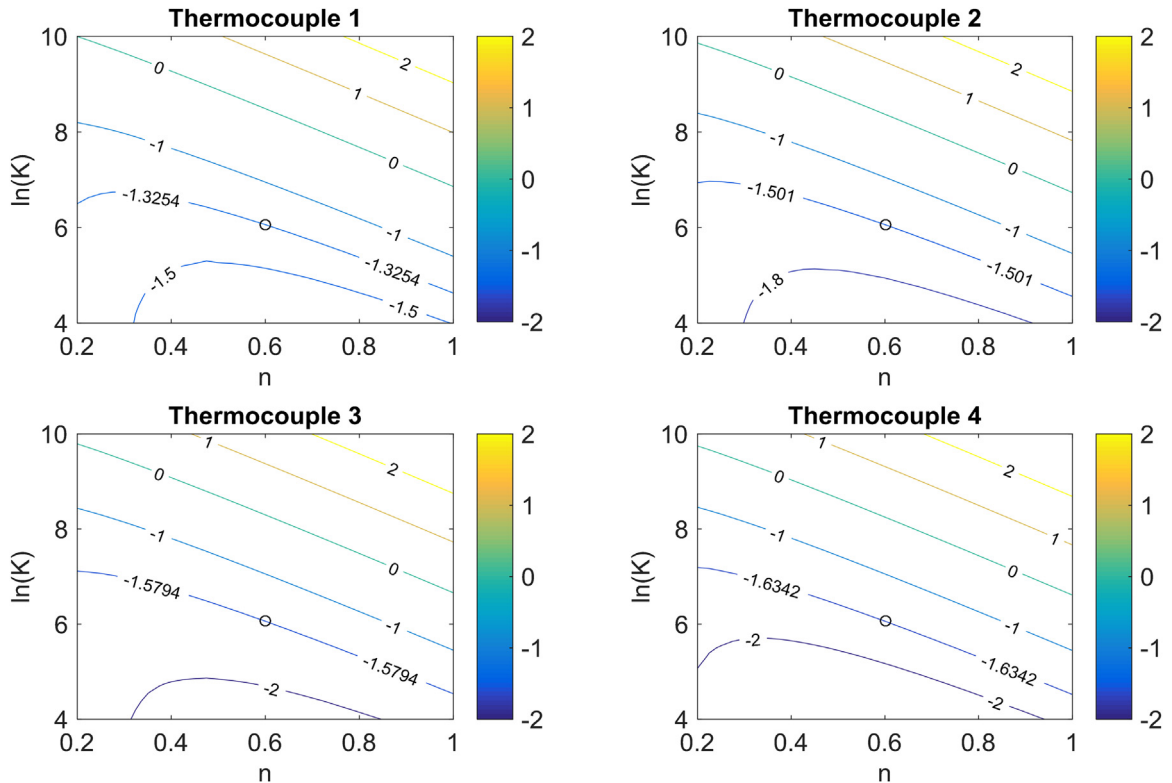
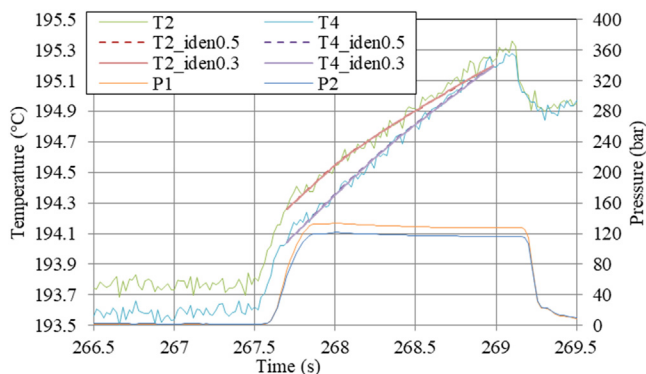


Fig. 9. Iso-lines of  $\ln(\Delta T)$  at the end of a two-second injection with an one-degree perturbation on the inlet temperature (the circled reference point :  $\ln(K) = 6.0625$ ;  $n = 0.6$ ), for thermocouples  $T_1, T_2, T_3$  et  $T_4$ .



**Fig. 10.** Measured temperature profiles and those calculated from identified viscosity parameters for an air shot at  $56.5 \text{ cm}^3 \cdot \text{s}^{-1}$  (« iden0.3 » for the identification with  $n_1$  fixed at 0.3; « iden0.5 » for the identification with  $n_2$  fixed at 0.5).

stant in space (on the inlet boundary of the direct model [17]) and in time.

Step 3 of the method is thus modified:

- Find the values of  $K_1$  and  $T_{in}$  which minimize the cost function  $J_v$  by inverse method, with the value of  $n_1$  fixed

because the sensitivity to the inlet temperature  $T_{in}$  is stronger when the value of  $n$  is small (For each isoline in Fig. 9, the smaller the value of  $n$ , the more curved the isoline is).

Step 4 of the method is also modified:

- Find the value of  $K_2$  which minimizes the cost function  $J_v$  by inverse method, with the value of  $n_2$  fixed and the value of  $T_{in}$  set to that identified in step 3.

In step 3, the Polak-Ribière's version of the conjugate gradient algorithm [23,24] coupled with the strong Wolfe criteria [25,26] is used to identify the values of  $K_1$  and  $T_{in}$ . In step 4, since there is only the value of  $K_2$  to identify, the one-dimension Newton's method is used.

#### 4.2.3. Validation of steps 1–4 of the viscous dissipation identification method

An example is given (Fig. 10) to show the measured temperature profiles along with the simulated temperature profiles from the identified  $K_1$  and  $K_2$  values. The example is based on an air shot at  $56.5 \text{ cm}^3 \cdot \text{s}^{-1}$  for a total volume of  $88.7 \text{ cm}^3$ . The material is PPC 9642. For the convenience of reading, only two of the four thermocouples  $T_{1-4}$  are shown.

In Fig. 10, « Ti\_iden0.3 » stands for the temperature profile of thermocouple  $T_i$ , calculated from  $K_1$  identified with  $n_1$  fixed at 0.3 (modified step 3 of the viscous dissipation identification method). Similarly, « Ti\_iden0.5 » corresponds to an identification of  $K_2$  with  $n_2$  fixed at 0.5 (modified step 4 of the viscous dissipation identification method).

The results of « iden0.3 » and « iden0.5 » are close to the measured (reference) temperature profiles, as they are on the same temperature isoline in the  $[n, \ln(K)]$  space. The identified  $K$ - $n$  pairs are  $9540.3-0.3$  and  $3917.6-0.5$ , respectively. We recall that there are an infinity of  $K$ - $n$  pairs to reproduce the same temperature measurements on the central axis (Here, we need two  $K$ - $n$  pairs to complete step 5 of the viscous dissipation identification method and obtain one critical point).

The pair  $3917.6-0.5$  is used to verify the sensitivity. If the value of  $K_2$  is incorrectly estimated and is 20% larger, i.e.  $4701.1 \text{ Pa} \cdot \text{s}^n$ , the calculated temperature profiles will be offset from the reference

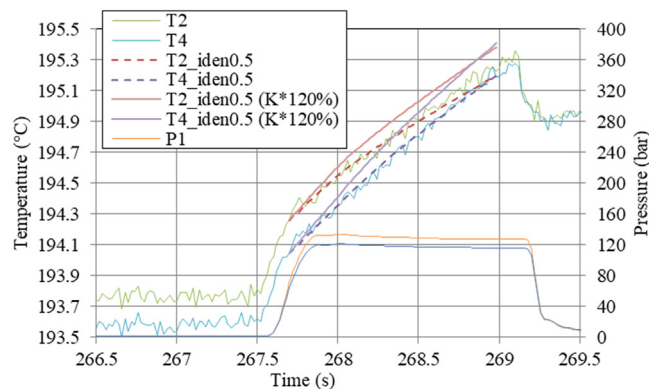


**Fig. 11.** Measured temperature profiles and those calculated from  $K_2$  values for an air shot at  $56.5 \text{ cm}^3 \cdot \text{s}^{-1}$  (« iden0.5 » for the identification with  $n_2$  fixed at 0.5; « K\*120% » for a value of  $K_2$  20% higher).

profiles. In Fig. 11, the temperature profiles calculated with a value of  $K_2$  20% larger ( $4701.1 \text{ Pa} \cdot \text{s}^n$ ) are labeled « K\*120% » and compared to the original temperature profiles.

It can be seen in Fig. 11 that the temperature profiles with  $K_2$  increased by 20% differ from the experimental measurements. The differences stand out in front of the measurement noise (of each thermocouple) having a standard deviation of 0.03 K. We can therefore confirm that the inverse method and the experimental conditions allow us to obtain  $K$ - $n$  pairs that minimize the cost function  $J_v$ .

#### 4.3. Viscosity identification results and discussion

Table 1 summarizes the inlet temperatures  $T_{in}$ ,  $K_1$  values (with  $n_1 = 0.3$ ) and  $K_2$  values (with  $n_2 = 0.5$ ) identified in the air shot tests of PPC 9642:

- with a setpoint temperature at  $195 \text{ }^\circ\text{C}$ 
  - for four different flow rate setpoints ( $14.1 \text{ cm}^3 \cdot \text{s}^{-1}$ ,  $28.3 \text{ cm}^3 \cdot \text{s}^{-1}$ ,  $42.4 \text{ cm}^3 \cdot \text{s}^{-1}$  and  $56.5 \text{ cm}^3 \cdot \text{s}^{-1}$ )
- with a setpoint temperature at  $205 \text{ }^\circ\text{C}$ 
  - for two different flow rate setpoints ( $42.4 \text{ cm}^3 \cdot \text{s}^{-1}$  and  $56.5 \text{ cm}^3 \cdot \text{s}^{-1}$ )

The volume of each air shot is the same. The duration is longer for air shots at lower flow rate.

By performing step 5 of the viscous dissipation identification method on each of these air shots at different flow rates, critical points can be obtained (Table 1).

It should be noted that for the same flow rate, the identified value of  $\dot{\gamma}_c$  should not change much [18]. In table 1, the value of  $\dot{\gamma}_c$  varies slightly for tests with the same flow rate setpoint. This variation is related to the numerical error of the inverse method (Fig. 8), to the duration of the measurement signals used in the inverse method [18] and also to the different initial temperature field and  $T_{in}$  in the finite element model for each test (because of the « slope bending effect » in Fig. 9).

In Fig. 12, the critical points of Polypropylene PPC 9642 are shown (with two setpoint temperatures at  $195 \text{ }^\circ\text{C}$  and  $205 \text{ }^\circ\text{C}$ ). Two viscosity curves (Cross-WLF model [27,28], at  $195 \text{ }^\circ\text{C}$  and  $205 \text{ }^\circ\text{C}$ ) of PPC 9642 from the « Autodesk® Moldflow® » software database are also presented in Fig. 12 for validation of the viscosity identification method. Two other Cross-WLF law curves of PPC 9642 at  $195 \text{ }^\circ\text{C}$  and  $205 \text{ }^\circ\text{C}$ , obtained by a rheometric nozzle (« Rheo-nozzle ») mounted on an injection molding machine [29,30], are also plotted in the same figure. We would like to highlight that the rheometric nozzle uses a pressure sensor to perform the viscosity measurement.

**Table 1**  
Summary of parameters identified for Polypropylene PPC 9642 air shot tests.

Flow rate setpoint (cm <sup>3</sup> .s <sup>-1</sup> )	T <sub>in</sub> (°C)	K <sub>1</sub> (Pa.s <sup>n</sup> )	K <sub>2</sub> (Pa.s <sup>n</sup> )	$\dot{\gamma}_c$ (s <sup>-1</sup> )	$\eta_c$ (Pa.s)
Setpoint temperature at 195 °C					
14.1	193.73	8310.2	4457.9	22.5	939.6
28.3	195.31	9353.8	4537.6	37.2	743.8
42.4	194.65	9111.8	4015.4	60.2	517.6
56.5	194.51	9540.3	3917.6	85.7	423.3
Setpoint temperature at 205 °C					
42.4	204.49	8187.3	3625.3	58.7	473.0
56.5	204.25	8648.5	3607.3	79.2	405.3

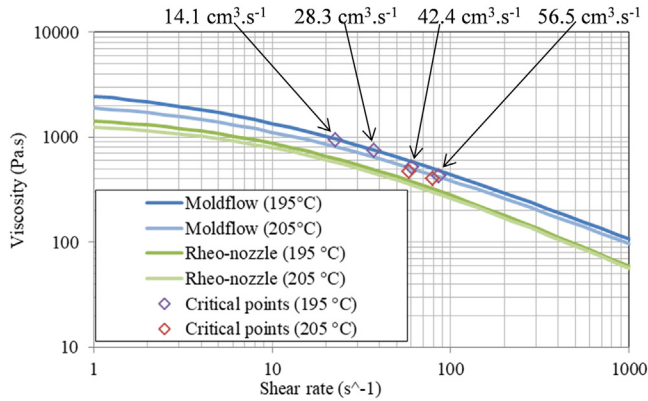


**Fig. 12.** Identified critical points of Polypropylene (PPC 9642) along with viscosity curves in the database of the software « Autodesk® Moldflow® » and viscosity curves identified by a rheometric nozzle [29,30] (« Rheo-nozzle »).

The Cross-WLF model [27,28] used in Fig. 12 is written as Eq. (11)

$$\eta = \frac{\eta_0}{1 + \left(\frac{\eta_0}{\tau^* \dot{\gamma}}\right)^{1-n}} \quad (11)$$

with  $\eta_0 = D_1 \exp\left(-\frac{A_1(T-T^*)}{A_2+(T-T^*)}\right)$ . And the parameters for PPC 9642 are shown in table 2.

The fact that the identified critical points are close to the « Moldflow » and « Rheo-nozzle » curves in Fig. 12 is encouraging for the validation of this new identification method.

We also note, in Fig. 12, that the viscosities resulting from the Cross-WLF law curves identified by the rheometric nozzle are lower than those of the « Autodesk® Moldflow® » software. Indeed, the temperature measurement at the wall of the rheometric nozzle is far from being representative of the melt temperature. Consequently, viscosity measurements with the rheometric nozzle, using capillary rheometry, do not take into account the increase in temperature of the polymer due to viscous dissipation in the capillary dies. When the temperature of the polymer is higher, the viscosity of the polymer decreases. The rheometric nozzle can therefore underestimate the viscosity by neglecting the increase in temperature of the polymer during the tests.

**Table 2**  
Cross-WLF model parameters in the database of the software « Autodesk® Moldflow® » and identified by a rheometric nozzle [29,30] for PPC 9642.

	Moldflow	Rheo-nozzle
A <sub>1</sub>	39.822	19.590
A <sub>2</sub> (K)	51.6	51.6
D <sub>1</sub> (Pa.s)	2.0935E+17	1.0410E+10
T* (K)	263.15	263.15
τ* (Pa)	19,996.2	19,100.0
n	0.3387	0.2600

When the setpoint temperature is increased to 205 °C, the critical points obtained are less viscous. In order to compare the identified viscosities at different setpoint temperatures (195 °C and 205 °C) with respect to the same critical shear rate, the identified critical points at 42.4 and 56.5 cm<sup>3</sup>.s<sup>-1</sup> (table 1, Fig. 12) are used to obtain a critical viscosity at  $\dot{\gamma}_c = 70$  s<sup>-1</sup> by interpolation for each setpoint temperature. The viscosity obtained by interpolation is noted as  $\eta_c^*$ . We obtain :

- $\eta_{c,195}^* = 474.6$  Pa.s for a setpoint temperature at 195 °C
- $\eta_{c,205}^* = 431.3$  Pa.s for a setpoint temperature at 205 °C.

The viscosity drops by 10% [ $(\eta_{c,195}^* - \eta_{c,205}^*)/\eta_{c,205}^*$ ] due to the temperature increase. According to the Cross-WLF model of « Moldflow », this ratio on the viscosity decrease is 14.8% for a shear rate at 70 s<sup>-1</sup>. According to the Cross-WLF model identified by the rheometric nozzle, this ratio is 6.4% for the same shear rate. The result obtained by the new viscous dissipation method is consistent with the « Moldflow » model and that obtained by the rheometric nozzle.

The same viscosity identification process is carried out for Polystyrene (ATOFINA LACQRENE® 1540), with a setpoint temperature at 195 °C and a flow rate of 14.1 cm<sup>3</sup>.s<sup>-1</sup>. The flow rate is set to a low value to avoid damaging the annular die with the flow of Polystyrene (ATOFINA LACQRENE® 1540) which is more viscous than Polypropylene (PPC 9642). The identified inlet temperature is 196.31 °C. The values of K<sub>1</sub> and K<sub>2</sub> are 18,591.5 and 10,223.5 Pa.s<sup>n</sup>, which lead to a critical viscosity value of 2292.5 Pa.s for a critical shear rate value of 19.9 s<sup>-1</sup>.

This result shows that, under the same air shot conditions, if PPC 9642 in the production line is replaced by LACQRENE® 1540, the identified critical viscosity value will become 2.4 times higher. The proposed method is able to measure the viscosity variation during polymer production, without using any pressure measurement.

## 5. Conclusion

The annular device (described in [17]) is used to measure temperature and pressure variations during air shot cycles on an injection molding machine. The results show that it is possible to detect a change in the polymer melt (PS impurity in PP) by directly reading the temperature curves measured on the central axis of the device, because a variation of the melt viscosity will lead to a change of viscous dissipation in the barrel and in the annular geometry.

Based on the viscous dissipation phenomenon described in [18], an inverse method is proposed to identify the viscosity and inlet temperature of polymer melts, by using temperature measurements on the central axis of the annular device. This method is tested on Polypropylene (PPC 9642) at two different temperatures. The identified critical viscosity points of PPC 9642 are consistent with the viscosity curves in the material database of the « Autodesk® Moldflow® » software and those identified in [29,30]. The proposed method is also able to measure the difference in viscos-

ity between Polypropylene (PPC 9642) and Polystyrene (ATOFINA LACQRENE® 1540).

Hence, this paper puts forward a new method of viscosity identification only based on temperature measurement and exploitation of invariant and critical values. It is all the more remarkable that the experiments are performed to detect and identify variations in viscosity under the real conditions of a polymer production line.

### Declaration of Competing Interest

The authors declare that they have no known competing financial interests or personal relationships that could have appeared to influence the work reported in this paper.

The authors declare the following financial interests/personal relationships which may be considered as potential competing interests:

Qiao LIN reports financial support was provided by French Government Ministry of Higher Education and Research and Innovation. Remi DETERRE reports equipment, drugs, or supplies was provided by TotalEnergies SE.

### CRediT authorship contribution statement

**Qiao Lin:** Writing – original draft, Methodology, Software, Investigation. **Nadine Allanic:** Writing – review & editing, Conceptualization, Project administration. **Pierre Mousseau:** Conceptualization, Supervision. **Manuel Girault:** Writing – review & editing, Software. **Rémi Deterre:** Conceptualization, Resources.

### Data availability

Data will be made available on request.

### Acknowledgement

This work was supported by the French Ministry of Higher Education, Research and Innovation and held in IUT Nantes.

This work used Polypropylene PPC 9642 kindly supplied by the company TotalEnergies.

### Supplementary materials

Supplementary material associated with this article can be found, in the online version, at doi:[10.1016/j.ijheatmasstransfer.2023.123954](https://doi.org/10.1016/j.ijheatmasstransfer.2023.123954).

### References

- [1] L. Hilliou, J.A. Covas, In-process rheological monitoring of extrusion-based polymer processes, *Polym. Int.* 70 (2021) 24–33, doi:[10.1002/pi.6093](https://doi.org/10.1002/pi.6093).
- [2] C. Abeykoon, Sensing technologies for process monitoring in polymer extrusion: a comprehensive review on past, present and future aspects, *Meas. Sens.* 22 (2022) 100381, doi:[10.1016/j.measen.2022.100381](https://doi.org/10.1016/j.measen.2022.100381).
- [3] J. Iwko, R. Wroblewski, R. Steller, Experimental study on energy consumption in the plasticizing unit of the injection molding machine, *Polimery* 63 (2018) 362–371 <https://bibliotekanauki.pl/articles/947526>. (accessed April 14, 2022).
- [4] J.Y. Chen, K.J. Yang, M.S. Huang, Online quality monitoring of molten resin in injection molding, *Int. J. Heat Mass Transf.* 122 (2018) 681–693, doi:[10.1016/j.ijheatmasstransfer.2018.02.019](https://doi.org/10.1016/j.ijheatmasstransfer.2018.02.019).
- [5] L. Saerens, C. Vervaet, J.P. Remon, T.D. Beer, Process monitoring and visualization solutions for hot-melt extrusion: a review, *J. Pharm. Pharmacol.* 66 (2014) 180–203, doi:[10.1111/jphp.12123](https://doi.org/10.1111/jphp.12123).

- [6] M. Karkri, Y. Jarny, P. Mousseau, Thermal state of an incompressible pseudo-plastic fluid and Nusselt number at the interface fluid–die wall, *Int. J. Therm. Sci.* 47 (2008) 1284–1293, doi:[10.1016/j.ijthermalsci.2007.11.009](https://doi.org/10.1016/j.ijthermalsci.2007.11.009).
- [7] Y. Wielhorski, P. Mousseau, Y. Jarny, D. Delaunay, N. Lefevre, Thermal balance between viscous heating and inlet thermal condition in non stationary polymer flow through a cylindrical die, *Int. J. Therm. Sci.* 50 (2011) 769–778, doi:[10.1016/j.ijthermalsci.2010.12.003](https://doi.org/10.1016/j.ijthermalsci.2010.12.003).
- [8] C. Abeykoon, P.J. Martin, A.L. Kelly, E.C. Brown, A review and evaluation of melt temperature sensors for polymer extrusion, *Sens. Actuators A Phys.* 182 (2012) 16–27, doi:[10.1016/j.sna.2012.04.026](https://doi.org/10.1016/j.sna.2012.04.026).
- [9] C. Abeykoon, A.L. Kelly, E.C. Brown, P.D. Coates, The effect of materials, process settings and screw geometry on energy consumption and melt temperature in single screw extrusion, *Appl. Energy* 180 (2016) 880–894, doi:[10.1016/j.apenergy.2016.07.014](https://doi.org/10.1016/j.apenergy.2016.07.014).
- [10] J. Vera-Sorroche, A.L. Kelly, E.C. Brown, P.D. Coates, Infrared melt temperature measurement of single screw extrusion, *Polym. Eng. Sci.* 55 (2015) 1059–1066, doi:[10.1002/pen.23976](https://doi.org/10.1002/pen.23976).
- [11] J. Launay, N. Allanic, P. Mousseau, R. Deterre, C. Plot, Effect of viscous dissipation in the prediction of thermal behavior of an elastomer cylindrical flow, *J. Mater. Process. Technol.* 252 (2018) 680–687, doi:[10.1016/j.jmatprotec.2017.10.035](https://doi.org/10.1016/j.jmatprotec.2017.10.035).
- [12] J. Launay, N. Allanic, P. Mousseau, R. Deterre, Y. Madec, Intrusive measurement of polymer flow temperature, *Polym. Eng. Sci.* 54 (2014) 2806–2814, doi:[10.1002/pen.23839](https://doi.org/10.1002/pen.23839).
- [13] J.A. Covas, J.M. Nóbrega, J.M. Maia, Rheological measurements along an extruder with an on-line capillary rheometer, *Polym. Test.* 19 (2000) 165–176, doi:[10.1016/S0142-9418\(98\)00086-5](https://doi.org/10.1016/S0142-9418(98)00086-5).
- [14] A. Kłodziński, P. Jakubowska, The application of an extrusion slit die in the rheological measurements of polyethylene composites with calcium carbonate using an in-line rheometer, *Polym. Eng. Sci.* 59 (2019) E16–E24, doi:[10.1002/pen.24941](https://doi.org/10.1002/pen.24941).
- [15] C. Pujos, N. Regnier, P. Mousseau, G. Defaye, Y. Jarny, Estimation of rheological law by inverse method from flow and temperature measurements with an extrusion die, *AIP Conf. Proc.* 908 (2007) 1287–1294, doi:[10.1063/1.2740987](https://doi.org/10.1063/1.2740987).
- [16] M. Girault, J. Launay, N. Allanic, P. Mousseau, R. Deterre, Estimation de la viscosité d'un polymère en écoulement à l'aide d'un modèle réduit, in: *Société Française de Thermique (SFT) 2018, 2018*.
- [17] Q. Lin, N. Allanic, P. Mousseau, Y. Madec, G. Beau, R. Deterre, On-line melt temperature measurements for polymer injection molding through an instrumented annular duct, *Polym. Eng. Sci.* 62 (2022) 3994–4004, doi:[10.1002/pen.26161](https://doi.org/10.1002/pen.26161).
- [18] Q. Lin, N. Allanic, R. Deterre, P. Mousseau, M. Girault, In-line viscosity identification via thermal-rheological measurements in an annular duct for polymer processing, *Int. J. Heat Mass Transf.* 182 (2022) 121988, doi:[10.1016/j.ijheatmasstransfer.2021.121988](https://doi.org/10.1016/j.ijheatmasstransfer.2021.121988).
- [19] W. Ostwald, About the rate function of the viscosity of dispersed systems, *Kolloid Z.* 36 (1925) 99–117.
- [20] A. de Waele, *Viscometry and plastometry*, *J. Oil Colour Chem. Assoc.* 6 (1923) 33–88.
- [21] R. Deterre, P. Mousseau, A. Sarda, *Injection Des polymères: simulation, Optimisation Et Conception*, Tec & Doc Lavoisier, France, 2003.
- [22] Q. Lin, N. Allanic, M. Girault, R. Deterre, P. Mousseau, A new solution for viscosity identification in a polymer production line via convection analysis, *Key Eng. Mater.* 926 (2022) 1914–1920, doi:[10.4028/p-05ji5t](https://doi.org/10.4028/p-05ji5t).
- [23] E. Polak, G. Ribiere, Note sur la convergence de méthodes de directions conjuguées, *Rev. Fr. Inform. Rech. Opér. Sér. Rouge.* 3 (1969) 35–43, doi:[10.1051/m2an/196903R100351](https://doi.org/10.1051/m2an/196903R100351).
- [24] J.R. Shewchuk, *An Introduction to the Conjugate Gradient Method Without the Agonizing Pain*, Carnegie-Mellon University, Department of Computer Science, 1994.
- [25] P. Wolfe, Convergence conditions for ascent methods, *SIAM Rev.* 11 (1969) 226–235.
- [26] P. Wolfe, Convergence conditions for ascent methods. II: some corrections, *SIAM Rev.* 13 (1971) 185–188.
- [27] M.M. Cross, Rheology of non-Newtonian fluids: a new flow equation for pseudoplastic systems, *J. Colloid Sci.* 20 (1965) 417–437.
- [28] M.L. Williams, R.F. Landel, J.D. Ferry, The temperature dependence of relaxation mechanisms in amorphous polymers and other glass-forming liquids, *J. Am. Chem. Soc.* 77 (1955) 3701–3707.
- [29] G.E.H. Sleiman, I. Petit, N. Allanic, S. Belhabib, Y. Madec, J. Launay, R. Deterre, Study of the rheological behavior of polypropylene/polyethylene extruded mixture using an instrumented die, *AIP Conf. Proc.* 1914 (2017) 040005, doi:[10.1063/1.5016715](https://doi.org/10.1063/1.5016715).
- [30] G. El Hajj Sleiman, Aptitude à La Mise En Oeuvre De Thermoplastiques Recyclés Et De biopolymère : Analyse Thermorhéologique De Mélanges PP/PE, These de Doctorat, 2018 Nantes <http://www.theses.fr/2018NANT4029> (accessed April 27, 2021).